Developmental Biology 455 (2019) 473–484

Contents lists available at ScienceDirect

Developmental Biology

journal homepage: www.elsevier.com/locate/developmentalbiology

Epigenetic factors Dnmt1 and Uhrf1 coordinate intestinal development

Julia Ganz [a,1,3], Ellie Melancon [a,3], Catherine Wilson [a], Angel Amores [a], Peter Batzel [a], Marie Strader [a], Ingo Braasch [a,1], Parham Diba [a,2], Julie A. Kuhlman [b], John H. Postlethwait [a], Judith S. Eisen [a,*]

[a] Institute of Neuroscience, 1254 University of Oregon, Eugene, OR, 97403, USA
[b] Department of Genetics, Development and Cell Biology, Iowa State University, Ames, IA, 50011, USA

ARTICLE INFO

Keywords:
Enteric nervous system
DNA methylation
Intestinal smooth muscle
Intestinal epithelium
Intestinal development
Hirschsprung disease

ABSTRACT

Intestinal tract development is a coordinated process involving signaling among the progenitors and developing cells from all three germ layers. Development of endoderm-derived intestinal epithelium has been shown to depend on epigenetic modifications, but whether that is also the case for intestinal tract cell types from other germ layers remains unclear. We found that functional loss of a DNA methylation machinery component, *ubiquitin-like protein containing PHD and RING finger domains 1 (uhrf1),* leads to reduced numbers of ectoderm-derived enteric neurons and severe disruption of mesoderm-derived intestinal smooth muscle. Genetic chimeras revealed that Uhrf1 functions both cell-autonomously in enteric neuron precursors and cell-non-autonomously in surrounding intestinal cells, consistent with what is known about signaling interactions between these cell types that promote one another's development. Uhrf1 recruits the DNA methyltransferase Dnmt1 to unmethylated DNA during replication. Dnmt1 is also expressed in enteric neurons and smooth muscle progenitors. *dnmt1* mutants have fewer enteric neurons and disrupted intestinal smooth muscle compared to wildtypes. Because *dnmt1*;*uhrf1* double mutants have a similar phenotype to *dnmt1* and *uhrf1* single mutants, Dnmt1 and Uhrf1 must function together during enteric neuron and intestinal muscle development. This work shows that genes controlling epigenetic modifications are important to coordinate intestinal tract development, provides the first demonstration that these genes influence development of the ENS, and advances *uhrf1* and *dnmt1* as potential new Hirschsprung disease candidates.

1. Introduction

Proper organ function requires coordinated development of multiple cell types over an appropriate temporal window. For example, development of a functioning intestinal tract involves coordination among intestinal epithelial cells derived from endoderm, muscle cells derived from mesoderm, and enteric neurons and glia derived from ectoderm. Cells from each of the three germ layers initially migrate and then proliferate, prior to their differentiation, which occurs essentially contemporaneously (Ganz, 2018; Ganz et al., 2016; Hao et al., 2016; Olden et al., 2008; Wallace et al., 2005a). Endoderm and mesoderm progenitor cells initially co-mingle (Gays et al., 2017; Warga and Nusslein-Volhard, 1999; Zorn and Wells, 2009), whereas the ectoderm that generates the neural crest cells that give rise to the enteric nervous system (ENS) is positioned far from the nascent endoderm and mesoderm. Thus, these ENS precursors must migrate for a significant distance to reach the developing intestinal tract before they can begin to differentiate and innervate it (Ganz, 2018; Lake and Heuckeroth, 2013). Signaling among these distinct cell types, or their progenitor cells, is critical for coordinated intestinal development. The intestinal epithelium influences development and differentiation of intestinal smooth muscle precursors (ISMPs) and intestinal smooth muscle cells (ISMCs), as well as development and differentiation of enteric precursor cells (EPCs) and the ENS (Fu et al., 2004; Korzh et al., 2011; Pietsch et al., 2006; Reichenbach et al., 2008; Sukegawa et al., 2000). The lateral plate mesoderm from which ISMPs and ISMCs arise influences intestinal epithelial development and EPC migration and

* Corresponding author.
E-mail address: eisen@uoregon.edu (J.S. Eisen).
[1] Present Address: Department of Integrative Biology, Michigan State University, 288 Farm Lane, East Lansing, MI, 48824.
[2] Present Address: Department of Pediatrics, Oregon Health & Science University, 3181 SW Sam Jackson Park Rd, Portland, OR, 97239.
[3] These authors contributed equally to this work.

https://doi.org/10.1016/j.ydbio.2019.08.002
Received 9 April 2019; Received in revised form 5 July 2019; Accepted 1 August 2019
Available online 5 August 2019

differentiation (Fu et al., 2004; Graham et al., 2017; Hao et al., 2016; Mwizerwa et al., 2011; Natarajan et al., 2002; Puzan et al., 2018; Reichenbach et al., 2008; Sukegawa et al., 2000). Similarly, the ENS regulates intestinal epithelial development and integrity (Neunlist et al., 2007, 2013; Puzan et al., 2018). Thus, there is interdependence of intestinal cell type development through signaling between progenitor cells of intestinal epithelium, smooth muscle, and ENS. Mutations in genes involved in development of any of these cell types can have profound and often deleterious consequences (Brosens et al., 2016; Goldstein et al., 2016; Wallace et al., 2005b; Yamamoto and Oda, 2015). For example, mutations in genes that regulate ENS development can result in disorders, such as Hirschsprung Disease (HSCR), in which the distal intestine is uninnervated and dysmotile (Heuckeroth, 2018).

A number of studies have revealed the importance of epigenetic modulation during development and functioning of the endodermal and mesodermal cell types that contribute to the intestinal tract (Elliott and Kaestner, 2015; Elliott et al., 2015; Jorgensen et al., 2018). For example, epigenetic modulation has been shown to be important for integrity of the intestinal epithelium (Marjoram et al., 2015) and proper development of intestinal smooth muscle (Jorgensen et al., 2018). Epigenetic modification via DNA methylation is a key regulator of the differential gene expression that underlies the ability of cells to develop distinct fates. DNA methylation patterns are established by the *de novo* DNA methyl transferases (Dnmt) 3a and 3b and maintained by Dnmt1 (Robertson and Wolffe, 2000). DNA methylation regulates intestinal epithelium formation by controlling the balance between cell proliferation and differentiation during development (Elliott and Kaestner, 2015; Marjoram et al., 2015; Sheaffer et al., 2014). Dnmt1 has also been shown to have an essential role in regulating intestinal smooth muscle differentiation, integrity, and survival (Jorgensen et al., 2018). DNA methylation has further been linked to ENS development because EPCs have decreased Dnmt expression in HSCR patients compared to controls and some HSCR patients have presumed pathogenic missense mutations in Dnmt3b (Torroglosa et al., 2014). Zebrafish mutants of *histone deacetlyase 1* (*hdac1)*, another epigenetic modifier gene, have fewer enteric neurons in addition to other neural crest defects (Ignatius et al., 2013). However, how epigenetic modifications, such as DNA methylation, affect ENS development remains poorly understood and it is also unclear how DNA methylation coordinates proper temporal development of the distinct cell types that coalesce to form the intestinal tract. Here, we investigate the role of epigenetic modulation on coordinated development of the intestinal tract by focusing on development of ectodermal derivatives that form the ENS and mesodermal derivatives that form the intestinal smooth muscle.

Dnmt proteins require partners to effect DNA methylation. For example, Dnmt1 is recruited by the modular protein Ubiquitin-like protein containing PHD and RING finger domains 1 (Uhrf1) to unmethylated DNA to maintain DNA methylation patterns after replication (Bestor, 2000; Bostick et al., 2007; Ooi and Bestor, 2008; Sharif et al., 2007). Zebrafish has been instrumental in elucidating the role of Uhrf1, as mouse mutants die early in development (Bostick et al., 2007; Muto et al., 2002; Sharif et al., 2007). Zebrafish *uhrf1* mutants show compromised intestinal barrier function resulting from disruption of the intestinal epithelium (Marjoram et al., 2015). They also show intestinal inflammation reminiscent of inflammatory bowel disease (Marjoram et al., 2015). However, little is known about how Uhrf1 influences ENS or intestinal smooth muscle cell development.

In this study, we examine the role of Uhrf1 and Dnmt1 in the coordination of intestinal development. To this end we analyze their effects on development of the ENS and intestinal muscle using a mutant *uhrf1* allele (*uhrf1*^{b1115}, hereafter referred to as *uhrf1*$^{-/-}$) that we isolated in a zebrafish forward genetic screen for mutants with changes in enteric neuron number (Kuhlman and Eisen, 2007). As previously reported, *uhrf1* mutants exhibit significant disruption of intestinal epithelial morphology (Marjoram et al., 2015). We demonstrate that they also exhibit severe disruption of intestinal smooth muscle and a variable reduction in enteric neuron number. This disruption of both EPCs and smooth muscle cells results in displacement of enteric neurons via both cell-autonomous and cell-non-autonomous mechanisms. We show that both *uhrf1* and *dnmt1* are expressed in EPCs and surrounding intestinal cell types, including intestinal smooth muscle. Consistent with the known interactions between Uhrf1 and Dnmt1, zebrafish *dnmt1* single mutants exhibit similar ENS and intestinal muscle phenotypes to *uhrf1* mutants. Our double mutant analysis demonstrated that Uhrf1 and Dnmt1 function together to regulate enteric neuron and intestinal smooth muscle development. This work provides evidence that genes controlling epigenetic modifications play an important role in coordination of intestinal development.

2. Materials and methods

2.1. Zebrafish husbandry

All zebrafish experiments were performed following protocols approved by the University of Oregon Institutional Animal Care and Use Committee. The *uhrf1*^{b1115} and *dnmt1*^{s904} mutations were propagated by mating heterozygous carriers to AB wildtypes. Homozygous *uhrf1*^{b1115} and *dnmt1*^{s904} single mutants were obtained by mating heterozygous carriers. Complementation testing was performed by mating adult zebrafish heterozygous for *uhrf1*^{b1115} and *uhrf1*^{hi272} (Sadler et al., 2007). Mutant larvae were first identified visually by smaller eyes and jaws and subsequently confirmed by fixing and staining with the pan-neuronal marker anti-Elavl and analyzing neuron numbers in the intestine. For some experiments, *uhrf1*^{b1115} and *dnmt1*^{s904} mutant carriers were outcrossed to *Tg(phox2b:EGFP)*^{w37} (Nechiporuk et al., 2007) and their progeny were grown up and screened for single and double mutant carriers that were subsequently crossed to visualize EPCs and neurons in living animals. *uhrf1*^{b1115} and *dnmt1*^{s904} single mutants had indistinguishable phenotypes. *uhrf1*^{b1115} and *dnmt1*^{s904} double mutants were generated by crossing heterozygotes to obtain a double mutant line.

Genotyping was performed on genomic DNA extracted from adult tails or heads obtained from larvae processed through immunohistochemistry. The *dnmt1*^{s904} mutation removes a *BslI* restriction site. A 230 bp PCR fragment containing the mutated site was amplified with forward 5'-TCTGTATCTTGTTTGCTCTGCTC-3' and reverse 5'-CTCACAGACACCACACCGT-3' primers. Digestion of the PCR product with *BslI* yielded two fragments in wildtype (185 and 45 bp) and did not cut the mutant PCR product. The *uhrf1*^{b1115} mutation creates a *HaeIII* restriction site. A 294 bp PCR fragment was amplified with forward 5'-AAGGGACGCCGAAGAAGAT-3' and reverse 5'GACGTTGTGTTGGCACTCTG-3' primers. Digestion with *HaeIII* generated three fragments in wildtypes (177, 94 and 23 bp) and four fragments (128, 94, 49 and 23 bp) in the presence of the mutation. Double mutants were genotyped using both assays.

2.2. RAD-tag genotyping

Previously we performed a forward-genetic screen to uncover regulators of neural crest development (Kuhlman and Eisen, 2007). One of the mutants identified, *b1115,* displayed a severe enteric neuron phenotype [Fig. 1A and B (Kuhlman and Eisen, 2007)]. Using Restriction site Associated DNA (RAD) sequencing of genomic DNA (Baird et al., 2008), we mapped the *b1115* genetic lesion to a 2.2 Mb region on chromosome 22. Phenotypic mutant and wildtype fish from a single-pair cross were identified by *phox2b:EGFP* transgene expression in the ENS at 5 days post fertilization (dpf) and five mutant or five wildtype individuals were pooled for sequencing. Genomic DNA was purified from the cross parents, from nine wildtype larval pools, and from 34 *b1115* mutant larval pools. RAD-tag libraries were prepared as described (Amores et al., 2011; Baird et al., 2008; Miller et al., 2007) and sequenced on an Illumina HiSeq 2000 to obtain 100-nucleotide single-end reads. We used Stacks version 1.19 (http://catchenlab.life.illinois.edu/stacks/) to organize

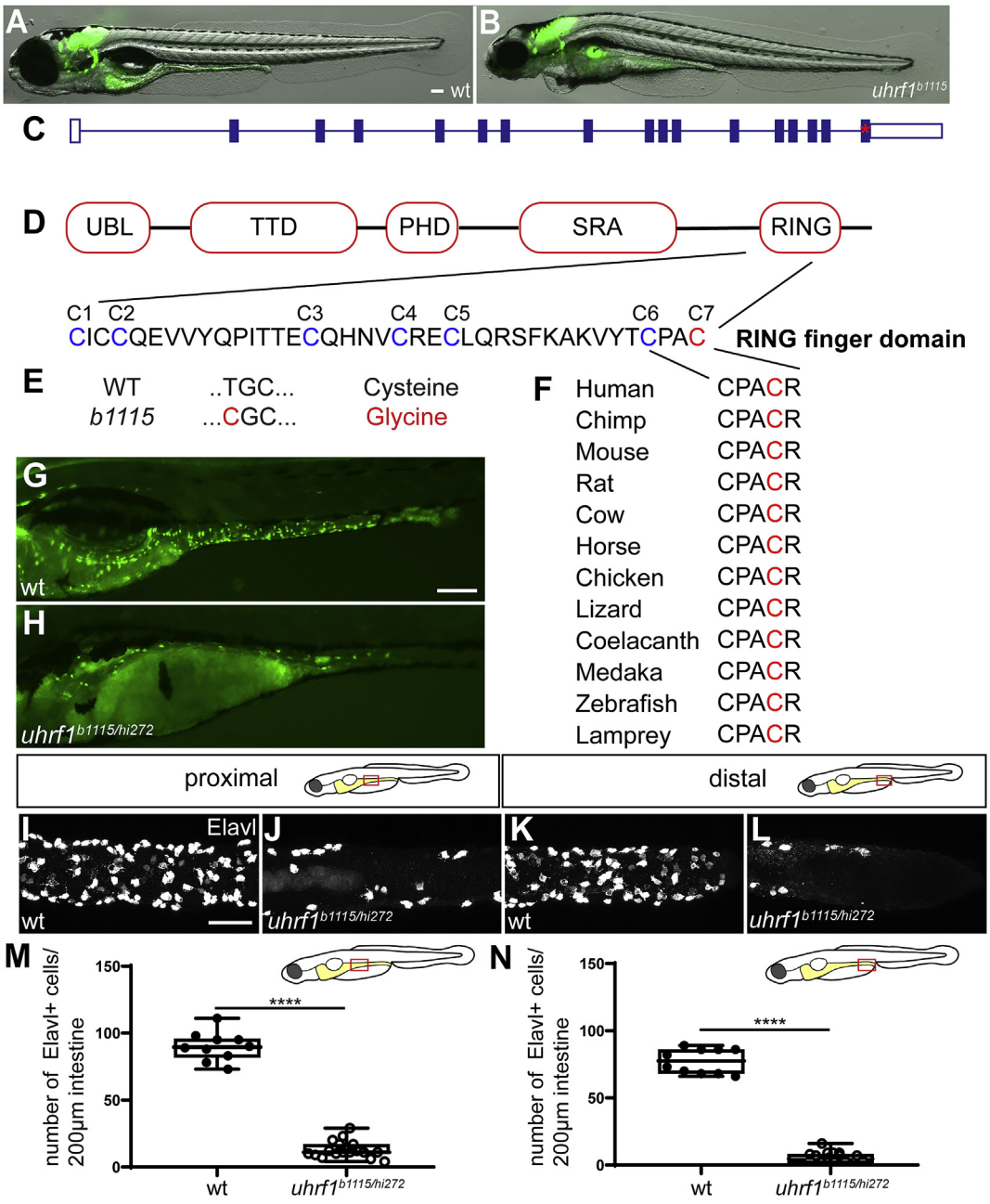

Fig. 1. The zebrafish *b1115* mutation has a non-synonymous single nucleotide polymorphism in an ultra-conserved amino acid of the RING domain of *uhrf1*. (A–B) Live images of 5 dpf wildtype (A) and *uhrf1*^{b1115} mutant (B) larvae show that mutants have smaller eyes and heart edema compared to wildtype siblings. (C) Exon 16 of *uhrf1* contains the mutation (red asterisk) in the *b1115* allele. (D) Schematic of important protein domains of *uhrf1* with a close-up of the seven conserved cysteines (Tauber and Fischle, 2015). (E) A non-synonymous single nucleotide polymorphism (T=>C) mutates the conserved cysteine 7 (red) to a Glycine. (F) Cysteine 7 (red) is conserved among phylogenetically diverse vertebrate species. (G) Complementation cross between the *b1115* allele and the *hi272* allele of *uhrf1* shows failure to complement in 5 dpf larvae as demonstrated by fewer *phox2b:EGFP* enteric neurons (green; H) compared to wildtype (green; G). In both proximal (J) and distal (L) intestine, *uhrf1*$^{b1115/hi272}$ mutants have fewer enteric neurons than wildtype siblings at 5 dpf (proximal I; distal K) as quantified in M and N. (M,N) Quantification of Elavl positive cells per 200 µm of proximal or distal intestine in wildtype or *uhrf1*$^{b1115/hi272}$ mutant [wildtype n = 10 (proximal), n = 10 (distal); *uhrf1*$^{b1115/hi272}$ n = 19 (proximal), n = 18 (distal)]. UBL, ubiquitin like; TTD, tandem tudor domain; PHD, plant homeodomain; SRA, SET and RING associated; PBR, polybasic region; RING, really interesting and new gene. A,B,G,H: side-views of whole-mount zebrafish larvae at 5 dpf. I–L: Confocal images of dissected intestines at 5 dpf. Scale bar = 100 µm in A,B,E,F; Scale bar = 50 µm in I-L. Unpaired *t*-test: **** = $p < 0.0001$.

reads into loci and to identify polymorphisms (Catchen et al., 2011, 2013). Illumina sequences were quality filtered with the process_radtags program of Stacks (Catchen et al., 2011, 2013) and aligned to the zebrafish genome (v. Zv9) (Howe et al., 2013) using GSNAP (Wu and Nacu, 2010). We ran pstacks with default parameters on the parent sequences, and with the parameters –bound_high .001 and –alpha .001 on pooled samples. The Stacks catalog was built from the parent sequences and sample stacks were matched to the catalog with sstacks. We excluded all loci with indels and more than two alleles in a single locus, and used the program SNPstats to calculate a G-test statistic comparing genotypes in mutants and wildtype pools (Hohenlohe et al., 2010). Sequences have been deposited in the Sequence Read Archive (https://www.ncbi.nlm.nih.gov/sra) under the accession number SRP118720.

Analysis of genes within the interval implicated *uhrf1* as a candidate

due to the similarities in phenotype between *uhrf1*^{b1115} and the previously described transgene insertion allele *uhrf1*^{hi272} (Amsterdam and Hopkins, 2004; Sadler et al., 2007). Crossing the *b1115* allele to the *hi272* allele resulted in non-complementation (Fig. 1G and H) indicating that *b1115* is a mutated allele of *uhrf1*. We quantified the number of ENS neurons in our complementation cross and found that the Elavl^{+} cells were significantly reduced in *uhrf1*$^{b1115/hi272}$ individuals compared to wildtype siblings in both proximal and distal intestine (Fig. 1I-N).To learn the site of the genetic lesion, we generated cDNA from pools of wildtype and mutant larvae, amplified and sequenced the *uhrf1* gene in each pool and performed sequence comparisons. We identified a single base pair change resulting in a cysteine-to-glycine change in amino acid 744, which lies in the zinc finger RING domain of the protein (Fig. 1C–E). Sequence analysis of vertebrate species in the conservation track of the human-centric 100-way species alignment in the UCSC Genome Browser (https://genome.ucsc.edu/; representative species shown in Fig. 1F) revealed that the affected amino acid is invariably conserved in all vertebrates in the alignment and that the affected cysteine (C7) is an essential part of the RING finger domain involved in binding of one of the zinc ions that are critical for the function of the RING finger domain (Fig. 1F) (Borden and Freemont, 1996).

2.3. Immunohistochemistry

Antibody staining for Elavl (1:10,000, Thermo Fisher Scientific, Eugene, OR, catalog number A-21271), GFP (1:1000, Thermo Fisher Scientific, Eugene, OR, A11122, catalog number A11120, nNOS (1:500, Santa Cruz Biotechnology, Santa Cruz, CA, catalog number sc-1025), 5-HT (1:10,000, Immunostar, Hudson, WI, catalog number 20080), Smooth muscle myosin (1:100, Alfa Aesar, catalog number J64817 BT-562), and Desmin (1:100, Sigma-Aldrich, catalog number D8281) was performed at 5 dpf as previously described (Uyttebroek et al., 2010). Immunostaining for Dnmt1 (1:250, Santa Cruz Biotechnology, Santa Cruz, CA, catalog number sc-20701) was performed on transverse cryosections of 48 hpf embryos expressing *phox2b:EGFP*. Staining with this antibody required a 5 min incubation in 3% H_2O_2/0.5% potassium hydroxide prior to standard staining methods. Antigens were visualized with standard fluorophore-labeled antibodies for rabbit IgG (1:1,000, Thermo Fisher Scientific, Eugene, OR, catalog number A-11008 or A-11071) and mouse IgG (1:1,000, Thermo Fisher Scientific, Eugene, OR, catalog number A-11001 or A-11030). DAPI staining was accomplished using ProLong Diamond Antifade Mountant with DAPI (Thermo Fisher Scientific; catalog number p36966).

2.4. Hematoxylin and eosin staining

Embryos were fixed in 4% paraformaldehyde and processed for paraffin sectioning and Hematoxylin and Eosin staining as previously described (Cheesman et al., 2011).

2.5. In situ hybridization

Embryos were fixed and processed for *in situ* hybridization as previously described (Seredick et al., 2012). Following *in situ* hybridization, embryos were embedded in agar, frozen, cryosectioned (Beattie and Eisen, 1997), and imaged on a confocal microscope as described below.

2.6. ENS transplantation

ENS transplantation was performed as previously described (Rolig et al., 2017). Briefly, donor embryos were labeled by injection of 5% tetramethylrhodamine dextran (3000 MW) at the 1–2 cell stage and reared until the next manipulation in filter-sterilized embryo medium (EM). Embryos at the 12–14 somite stage were mounted in agar, a small hole dissected in the skin, and cells transplanted as previously described (Eisen, 1991). At 5 dpf, hosts and donors were fixed in 4% paraformaldehyde in 1 × PBS for 3 h at room temperature and then washed 3 × 10 min in 1 × PBS. We performed immunohistochemistry with anti-Elavl and anti-GFP (see immunohistochemistry section) to reveal both host and donor-derived enteric neurons.

2.7. Image acquisition

Confocal images were acquired on a Zeiss Pascal confocal microscope using a 40X water immersion objective and AIM or ZEN software (Carl Zeiss Microscopy, LLC, Thornwood, New York, USA) or a Leica SP8 confocal microscope using a 40X water immersion objective or a 63X oil immersion objective, 405-diode, white light lasers and LASX software, or a Leica TCSSPE confocal microscope using a 40X oil immersion objective and LASX software. Low magnification images were acquired using a Leica MZ205 FA fluorescent stereomicroscope and LAS software. Images were processed and analyzed using Photoshop CC (Version 19.1.1, Adobe Systems, Inc., San Jose, CA, USA) and FiJi software to adjust contrast.

2.8. Image analysis

Following immunohistochemistry, intestines were dissected and mounted in PBS between two coverslips. For cell quantification, projections along the y-axis were generated from confocal stacks in ZEISS LSM Image browser and used for manual cell counts and colocalization analysis between Elavl and nNOS or Elavl and 5-HT. Counts were performed in proximal intestine, defined as extending 200 μM from the caudal end of the intestinal bulb, and in the distal intestine, defined as extending 200 μM proximal to the anus. Alternatively, confocal stacks were loaded into Imaris (Version 9.2.1), appropriate regions of interest were selected, estimated cell diameter was set to 5.38 μm, spot selection was checked for appropriate threshold levels, and cell counts were manually verified. To determine significant differences, we performed an unpaired *t*-test using GraphPad Prism 8.01. For multiple comparisons, we performed One-way Anova followed by Tukey's post-hoc test using GraphPad Prism 8.01.

3. Results

3.1. Zebrafish uhrf1 mutants have fewer enteric neurons

uhrf1^{b1115} was originally isolated from a forward genetic screen for mutations affecting ENS development (Kuhlman and Eisen, 2007) based on a decrease in the number of ENS neurons in larvae. The line has been maintained for over a decade by outcrossing to AB. The *uhrf1*^{b1115} mutation was identified using RAD-mapping, as described in the Methods and confirmed by non-complementation with another allele of *uhrf1* (*hi272*) that has been shown to have strongly reduced CG DNA methylation (Fig. 1G-N, Table 1) (Feng et al., 2010; Sadler et al., 2007). Larvae

Table 1
Complementation scoring of *uhrf1*^{b1115} heterozygous carriers crossed to *uhrf1*^{hi272} heterozygous carriers shows that *b1115* and *hi272* are both mutant alleles of *uhrf1*.

Pair #	Female	Male	Wildtype	*b1115/hi272*	Total	% Mutants
1	*hi272*	*b1115*	90	40	130	31
2	*hi272*	*b1115*	88	24	112	21
3	*hi272*	*b1115*	81	41	122	34
4	*hi272*	*b1115*	137	38	175	22
5	*hi272*	*b1115*	100	33	133	25
6	*b1115*	*hi272*	75	24	99	24
7	*b1115*	*hi272*	112	46	158	29
8	*b1115*	*hi272*	126	48	174	28
9	*b1115*	*hi272*	16	7	23	30
10	*b1115*	*hi272*	42	13	55	24
11	*hi272*	*b1115*	12	3	15	20
12	*hi272*	*b1115*	13	4	17	24
Total			**892**	**321**	**1213**	**26**

show the smaller eye phenotype that has previously been described for 5 dpf *uhrf1* mutants (Fig. 1A and B) (Tittle et al., 2011). There are several additional *uhrf1* mutant alleles that have also been demonstrated to decrease DNA methylation (Marjoram et al., 2015; Tittle et al., 2011).

To learn about the role of Uhrf1 in ENS development, we examined five time points spanning different stages of enteric progenitor cells (EPC) migration and ENS neuron specification using the *phox2b:EGFP* transgenic line that expresses in enteric neurons and their precursors (Taylor et al., 2016). At 30–32 h post fertilization (hpf), *phox2b:EGFP*$^{+}$ EPCs enter the rostral intestine and migrate caudally, reaching the distal end at around 66 hpf. ENS neurogenesis starts around 48 hpf rostrally and continues caudally until a functional ENS has formed at 5 dpf (Olden et al., 2008; Shepherd et al., 2004). At 48 and 57 hpf, EPC migration in *uhrf1* mutant embryos is indistinguishable from wildtype siblings (data not shown). At 72 and 96 hpf, fewer *phox2b:EGFP*$^{+}$ cells are present in *uhrf1* mutants compared to their wildtype siblings (Fig. 2), but the ENS phenotype is variable in *uhrf1* mutants. At 5 dpf, the reduction in *phox2b:EGFP*$^{+}$ ENS neurons is significant and robust (Figs. 3 and 4). To investigate the ENS phenotype in more detail at 5 dpf, we examined the number of ENS neurons in proximal and distal intestine using immunohistochemistry with the pan-neuronal marker Elavl (Fig. 4). At this stage, there are two main neuronal subtypes, those expressing neuronal nitric oxide synthase (nNOS) and those expressing serotonin (5-HT) that together comprise about 80% of ENS neurons (Uyttebroek et al., 2010). A change in the number of ENS neurons could reflect a change in either one or both of these subtypes. We counted the overall number of neurons using an antibody to Elavl which is expressed in all ENS neurons (Kuhlman and Eisen, 2007), as well as antibodies to these two neurotransmitters (Uyttebroek et al., 2010). We found that the overall number of ENS neurons was significantly reduced in both proximal and distal intestine, as a result of reductions in both subtypes, indicating that *uhrf1* does not differentially affect specification of these neuronal subtypes (Fig. 4). Notably, ENS neurons were essentially absent from the distal-most 200 μm of the intestine (Fig. 3D; Fig. 4D,H,I-K). This phenotype is not due to a developmental delay, as mutant larvae die around 7 dpf still displaying the mutant ENS phenotype observed at 5 dpf.

3.2. Enteric progenitors and surrounding intestinal cells express uhrf1 and dnmt1

As a first step toward elucidating the role of *uhrf1* in the developing intestinal tract, we examined the *uhrf1* expression pattern by *in situ* hybridization. Expression of *uhrf1* has been documented in zebrafish embryos in developing endoderm (Sadler et al., 2007). Previous studies showed that Uhrf1 is required for normal development of the intestinal epithelium in zebrafish, but did not investigate its role in development of other intestinal cell types such as intestinal smooth muscle cells or ENS neurons (Marjoram et al., 2015). EPCs, endoderm, and developing mesoderm are in such close proximity during intestinal development (Wallace et al., 2005a) that previous studies did not differentiate the expression pattern of *uhrf1* among these cell types. The transgene Tg(*phox2b:EGFP*) is expressed in migrating EPCs beginning around 30–32 hpf (Shepherd et al., 2004; Taylor et al., 2016), allowing identification of EPCs among surrounding intestinal cells. We tested several commercially available antibodies against Uhrf1 using a variety of antigen retrieval methods, but none of them showed specific staining at relevant developmental stages. Thus, we evaluated *uhrf1* mRNA expression in embryos homozygous for the *phox2b:EGFP* transgene at 48 hpf and performed immunohistochemistry to detect GFP expression in EPCs (Fig. 5A). Similar to Sadler et al. (2007), we observed *uhrf1* transcript in the tectum, retina, branchial arches, and developing endoderm (Fig. 5A and data not shown). We also observed *uhrf1* expression in *phox2b:EGFP*-positive EPCs and surrounding intestinal cells including ISMPs, suggesting that *uhrf1* plays a role in both ENS and intestinal smooth muscle development (Fig. 5A), as well as in intestinal epithelium development, as previously shown (Marjoram et al., 2015).

Uhrf1 is necessary to recruit Dnmt1 to unmethylated DNA during replication (Bostick et al., 2007; Muto et al., 2002; Sharif et al., 2007) and zebrafish *dnmt1*^{s904} mutants exhibit hypomethylation (Anderson et al., 2009). Because Dnmt1 is necessary to maintain intestinal epithelial progenitor cells (Elliott et al., 2015) and expression of Dnmt1 has been documented in zebrafish embryos in developing endoderm (Liu et al., 2015; Rai et al., 2006), we wondered whether Dnmt1 protein is also expressed in EPCs and surrounding intestinal cell types. To address this question, we immunostained transverse sections of *phox2b:EGFP*-expressing embryos at 48 hpf with a Dnmt1 antibody. Our results identified Dnmt1-positive EPCs migrating within the Dnmt1-positive population of endodermal cells and ISMPs that prefigure the intestinal epithelium (Fig. 5B). We conclude that EPCs and ISMPs express both *uhrf1* and *dnmt1*. We note, however, that there are also cells surrounding the nascent intestine that are negative for Dnmt1 or *uhrf1* (Fig. 5).

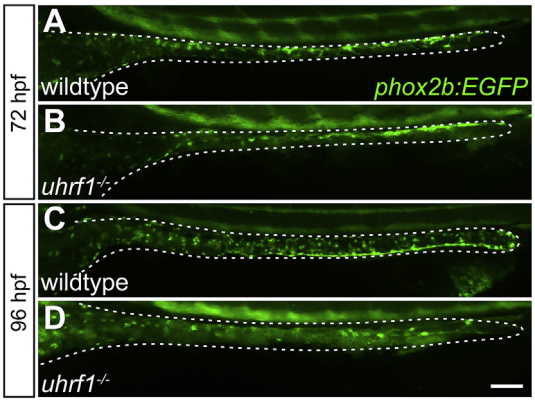

Fig. 2. The *uhrf1* mutant ENS progenitor phenotype emerges around 72 hpf. Whole-mount side views of wildtype (A,C) and *uhrf1* mutants (B,D). *uhfr1* mutants have fewer *phox2b:EGFP* positive cells (green) than wildtype siblings at 72 hpf (A,B) and 96 hpf (C,D). Scale bar = 100 μm.

3.3. Epigenetic modifiers Uhrf1 and Dnmt1 function together during intestinal tract development

The expression patterns of *dnmt1* and *uhrf1* showed that they are expressed in the same cells at the same time, suggesting that Uhrf1 and Dnmt1 function together during establishment of the intestinal tract. To test this hypothesis, we first analyzed ENS development in *dnmt1* mutants at the same five time points at which we analyzed *uhrf1* mutants (Fig. 6) and then we analyzed *uhrf1*;*dnmt1* double mutants.

dnmt1^{s904}, the mutation we used for our studies, was isolated from an ENU mutagenesis screen for regulators of pancreas development. We have maintained this allele, a splice acceptor mutation resulting in a complete loss of Dnmt1 catalytic activity (Anderson et al., 2009), on an AB background carrying *phox2b:EGFP*. As in *uhrf1* mutants, EPC migration in *dnmt1* mutant embryos is indistinguishable from wildtype siblings at 48 and 57 hpf (data not shown). At 72 and 96 hpf, fewer *phox2b:EGFP*$^{+}$ cells are present in *dnmt1* mutants compared to their wildtype siblings (Fig. 6), but as in *uhrf1* mutants the reduction in *phox2b:EGFP*$^{+}$ cells is strongest and most robust at 5 dpf (Fig. 7C, G). We then quantified the number of enteric neurons in *dnmt1*^{s904} and *uhrf1* mutants at 5 dpf. *dnmt1* and *uhrf1* mutant larvae both exhibited reductions in ENS neurons that were statistically the same, and significantly different from wildtype larvae (Fig. 7A–C, E-G). To further test interactions between Dnmt1 and Uhrf1, we crossed *dnmt1*;*uhrf1* double heterozygotes into a Tg(*phox2b:EGFP*) line and examined enteric neuron number. These double mutants displayed the same ENS phenotype as *uhrf1* and *dnmt1* single mutants (Fig. 7D,H). Quantification revealed that enteric neuron number was the same in both single and double mutants and significantly different from wildtypes (Fig. 7I and J), consistent with the hypothesis

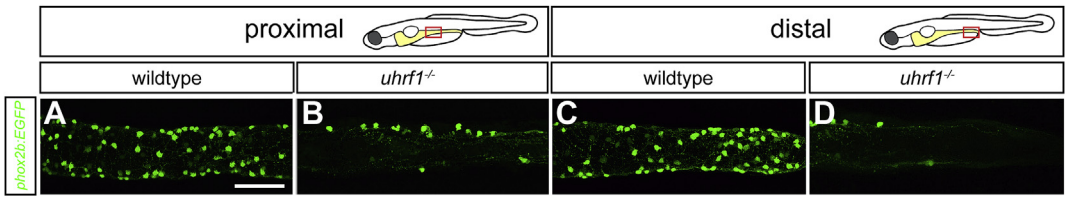

Fig. 3. *uhrf1* mutants have fewer neurons in both proximal and distal intestine. Confocal images of dissected intestines of wildtype (A,C) and *uhrf1* mutants (B,D). *uhfr1* mutants have fewer *phox2b:EGFP* positive enteric neurons (green) than wildtype siblings at 5 dpf (A,C) in both proximal (B) and distal (D) intestine. Scale bar = 50 μm.

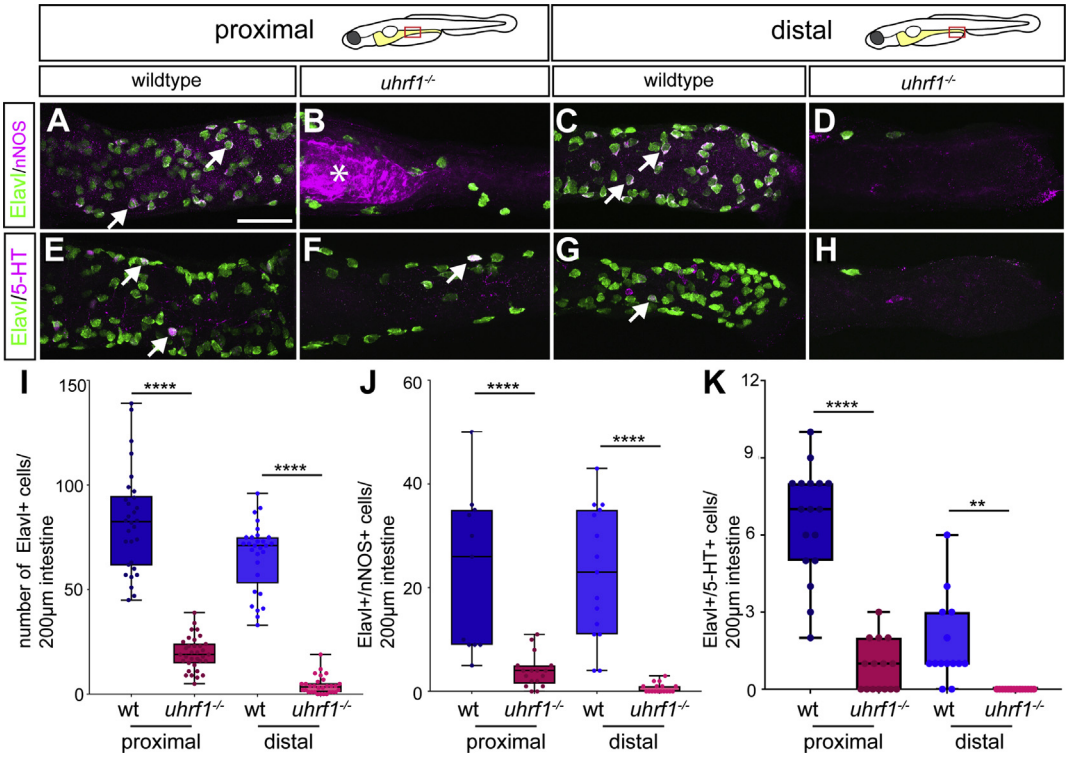

Fig. 4. Both of the major ENS neuronal subtypes are reduced in *uhrf1* mutants. Confocal images of dissected intestines from wildtypes (A,C,E,G) and *uhrf1* mutants (B,D,F,H) stained for expression of the pan-neuronal marker Elavl, and either nNOS or 5-HT. In both proximal (B,F) and distal (D,H) intestine, *uhrf1* mutants have fewer enteric neurons than wildtype siblings at 5 dpf (proximal A,E; distal C,G) as quantified in (I). Both nNOS and 5-HT expressing ENS neuronal subtypes show similar reductions at 5 dpf [Elavl (green), nNOS or 5-HT (magenta)] as quantified in (J,K). Arrows point to examples of nNOS or 5-HT positive neurons. (I) Quantification of Elavl positive cells per 200 μm of proximal or distal intestine in wildtype (blue) or mutant (red) [wildtype n = 30 (proximal), n = 29 (distal); $uhrf1^{-/-}$ n = 29 (proximal), n = 30 (distal)]. (J–K) Quantification of Elavl and nNOS (J) and 5-HT (K) positive cells per 200 μm proximal or distal intestine in wildtype (blue) and mutant (red) [nNOS: wildtype n = 11 (proximal), n = 15 (distal); $uhrf1^{-/-}$ n = 17 (proximal), n = 17 (distal); 5-HT: wildtype n = 17 (proximal), n = 14 (distal); $uhrf1^{-/-}$ n = 15 (proximal), n = 13 (distal)]. Asterisk in B indicates autofluorescent background common to *uhrf1* mutant intestines. Scale bar = 50 μm in A-H. Unpaired *t*-test: **** = $p < 0.0001$; ** = $p < 0.01$.

that Uhrf1 and Dnmt1 act together during ENS development.

Homozygous *uhrf1* mutants were previously shown to have disrupted intestinal epithelium development (Marjoram et al., 2015). We found that *uhrf1* is expressed in ISMPs, prompting us to test whether *uhrf1* mutants also show altered development of intestinal smooth muscle. We analyzed smooth muscle development in 5 dpf whole-mount *uhrf1* mutants and found that both longitudinal and circumferential intestinal smooth muscle fibers were essentially absent (Fig. 8A–D). Cross-sections stained with neuronal and smooth muscle markers or with Hematoxylin and Eosin (HE) revealed severe disruption of both intestinal smooth muscle and ENS components (Fig. 8E-L). They also showed that, instead of being sandwiched between the longitudinal and circumferential smooth muscle cell layers, cell bodies of enteric neurons of *uhrf1* mutants often appeared to be 'floating' at some distance from the intestinal epithelium (Fig. 8H, arrow). Although this aspect of the phenotype is subtle and difficult to quantify, many of these neurons had a more rounded appearance than those of wildtypes, consistent with not being located between two closely apposed muscle layers.

Dnmt1 has an essential role in smooth muscle cell development in mouse and humans (Jorgensen et al., 2018). To test whether this role of Dnmt1 is conserved, we examined intestinal smooth muscle development in zebrafish *dnmt1* mutants. We found that, like *uhrf1* mutants, *dnmt1* mutants had severely disrupted intestinal smooth muscle development (Fig. 9). In addition, enteric neurons of *dnmt1* mutants shared the same subtle morphological phenotypes as those of *uhrf1* mutants.

The experiments described in this section show that *uhrf1* and *dnmt1* mutants have indistinguishable intestinal smooth muscle and enteric neuron phenotypes. Previous work showed that these two mutants also have the same intestinal epithelial phenotypes (Marjoram et al., 2015). Together these studies support the conclusion that Uhrf1 and Dnmt1 function in the same pathway and together control normal establishment of the intestinal tract by regulating development of each of the constituent cell types.

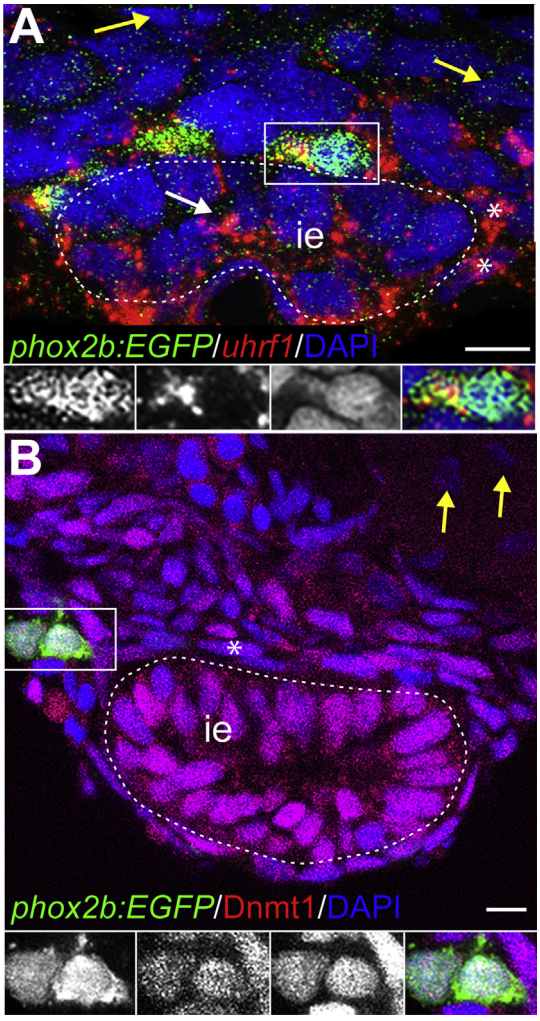

Fig. 5. *uhrf1* and Dnmt1 are expressed in enteric, epithelial, and smooth muscle progenitors during development. Transverse sections of stained embryos. (A) At 48 hpf, *uhrf1* (red) is expressed in *phox2b:EGFP* (green) positive EPCs and also in DAPI-positive (blue) ISMPs (asterisks) and epithelial progenitors (white arrow). Yellow arrows point to *uhrf1* negative cells outside of the nascent intestine. White dashed line indicates intestinal epithelium (ie). Insets show enlargement of cell (white box), GFP, *uhrf1*, DAPI, and overlay from left to right. Note that the GFP staining appears speckled due to the RNA *in situ* hybridization procedure. (B) At 48 hpf, Dnmt1 (red) is expressed in *phox2b:EGFP* (green) positive EPCs and in DAPI-positive (blue) ISMPs (asterisk). Insets show enlargements of outlined cell, GFP, Dnmt1, DAPI and overlay from left to right. Yellow arrow points to Dnmt1 negative cell outside of the intestine. Scale bar = 10 μm in A-B.

3.4. Genetic chimeras reveal that uhrf1 functions both cell-autonomously and cell-non-autonomously in ENS development

EPCs, smooth muscle precursors, and intestinal epithelial precursors are intermingled during development and previous studies have shown that signals among these nascent intestinal constituents are critical for proper differentiation of each cell type (Fu et al., 2004; Graham et al., 2017; Hao et al., 2016; Korzh et al., 2011; Mwizerwa et al., 2011; Natarajan et al., 2002; Neunlist et al., 2007, 2013; Olden et al., 2008; Pietsch et al., 2006; Puzan et al., 2018; Reichenbach et al., 2008; Sukegawa et al., 2000). Cells of all three germ layers express *uhrf1* during intestinal development, raising the possibility of cell-non-autonomous interactions. To learn whether loss of Uhrf1 disrupts interactions between cells derived from the different germ layers, we focused on EPCs in genetic chimeras in which the ENS was wildtype and the intestinal

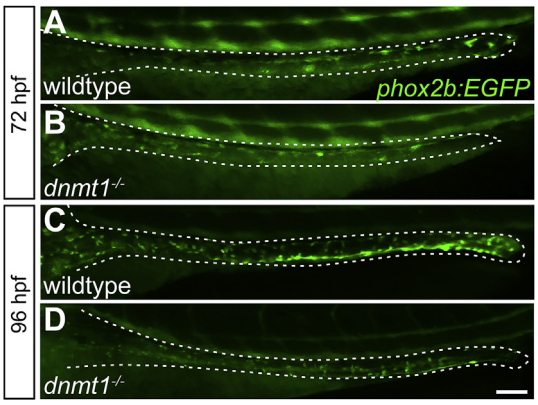

Fig. 6. The *dnmt1* mutant ENS progenitor phenotype emerges around 72 hpf. Whole-mount side views of wildtype (A,C) and *dnmt1* mutants (B,D). *dnmt1* mutants have fewer *phox2b:EGFP* positive cells (green) than wildtype siblings at 72 hpf (A,B) and 96 hpf (C,D). Scale bar = 100 μm.

epithelium and muscle were mutant for *uhrf1*. We generated chimeras by transplanting vagal neural crest that generates the ENS from *phox2b:EGFP*-expressing wildtype donors into host embryos from an incross of heterozygous *uhrf1* mutants. Thus, some hosts were wildtype, some were heterozygous, but phenotypically wildtype, and some were homozygous mutant (Fig. 10A and B). In this experimental set-up, all GFP-positive enteric neurons were donor-derived. As predicted, wildtype EPCs transplanted into phenotypically wildtype hosts contributed to the ENS along the entire length of the intestinal tract (Fig. 10D). Notably, the GFP-positive enteric neurons are intermingled with unlabeled, host-derived enteric neurons. In the context of a *uhrf1* mutant host environment, wildtype donor enteric neurons were distributed along most of the intestinal tract. Because there are so few enteric neurons in *uhrf1* mutants, transplanted wildtype EPCs have the potential to proliferate more than they would in wildtypes, where they compete with the native EPCs (Rolig et al., 2017; Troll et al., 2018). Despite being present along most of the intestine, wildtype enteric neurons were specifically absent from the distal-most region of the intestine in *uhrf1* mutants (Fig. 10E, asterisk, 5/5). This result is consistent with the idea that Uhrf1 function is necessary cell-non-autonomously for EPCs to migrate far enough caudally to populate the distal portion of the intestinal tract.

Because *uhrf1* is expressed in EPCs, we also tested whether Uhrf1 function is required cell-autonomously. We performed the same transplantation as described above, but transplanted vagal neural crest from labeled donor embryos derived from a *uhrf1* mutant incross carrying the *phox2b:EGFP* transgene into unlabeled wildtype hosts (Fig. 10A,C). As in the previous experiment, wildtype donor cells transplanted into wildtype hosts populated the entire length of the intestine (Fig. 10D). In contrast, in most cases mutant donor EPCs migrated only a short distance caudally after entering the wildtype host intestine (4/5). Even in the single case in which transplanted *uhrf1* mutant cells reached the distal intestine (1/5), the mutant donor cells did not proliferate as much as wildtype precursors (Fig. 10F). This result provides evidence that Uhrf1 function is required cell-autonomously in EPCs for them to migrate and proliferate normally.

4. Discussion

This study provides evidence that disruption of DNA methylation factors interrupts the developmental trajectories of the three germ layers that contribute to the intestinal tract, thus preventing formation of a functional organ. Previous studies demonstrated that derivatives of these germ layers, intestinal epithelium, intestinal smooth muscle, and the ENS develop over a similar time frame. Importantly, cells derived from these germ layers provide signals that are critical for one another's differentiation (Fig. 11) (Fu et al., 2004; Graham et al., 2017; Hao et al., 2016; Korzh et al., 2011; Mwizerwa et al., 2011; Natarajan et al., 2002; Neunlist

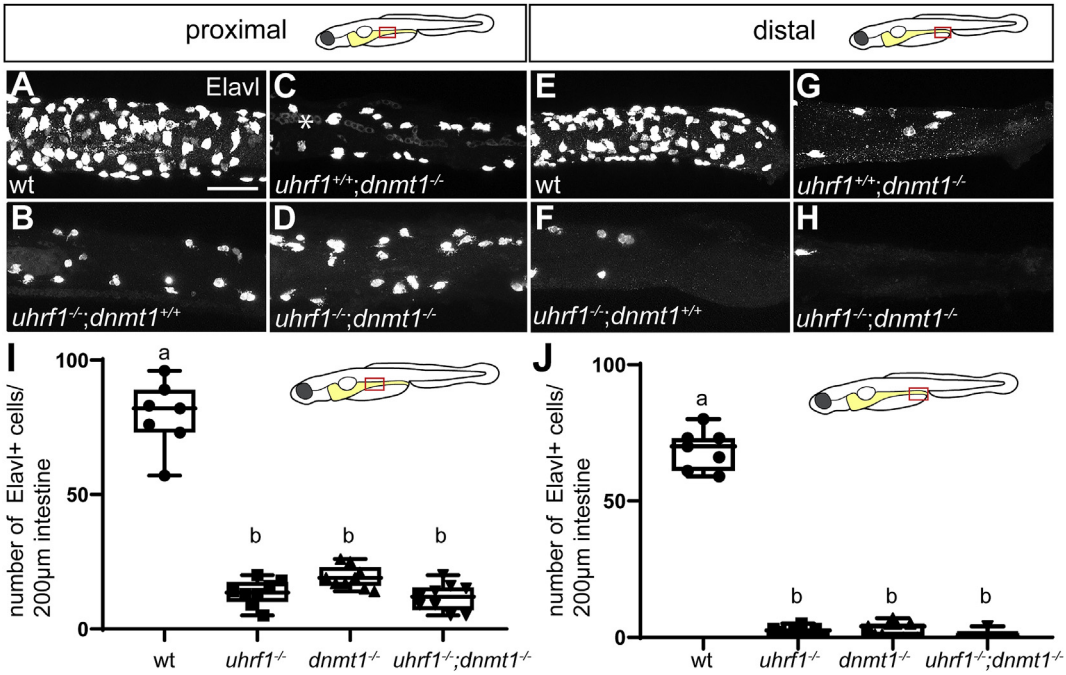

Fig. 7. *uhrf1;dnmt1* double mutants show similar reduction in enteric neurons compared to *uhrf1* and *dnmt1* single mutants. Confocal images of dissected 5 dpf intestines of wildtypes (A,E) and *uhrf1* (B,F), *dnmt1* (C,G) and *uhrf1;dnmt1* (D,H) mutants. In both proximal and distal intestine, single and double mutants show a similar reduction in Elavl positive enteric neurons (white) compared to wildtype siblings. Quantification of Elavl positive cells per 200 µm in proximal (I) or distal (J) intestine at 5 dpf in wildtype (wt), *uhrf1*$^{-/-}$, *dnmt1*$^{-/-}$ and *uhrf1*;*dnmt1* double mutants [wildtype n = 7 (proximal), n = 7 (distal); *uhrf1*$^{-/-}$ n = 8 (proximal), n = 8 (distal); *dnmt1*$^{-/-}$ n = 9 (proximal), n = 9 (distal); *uhrf1*$^{-/-}$;*dnmt1*$^{-/-}$ n = 9 (proximal), n = 9 (distal)]. Larvae were genotyped as described in the Methods section. One-way Anova followed by Tukey's post-hoc test, letters indicate $P < 0.0001$. A–H: Scale bar = 50 µm.

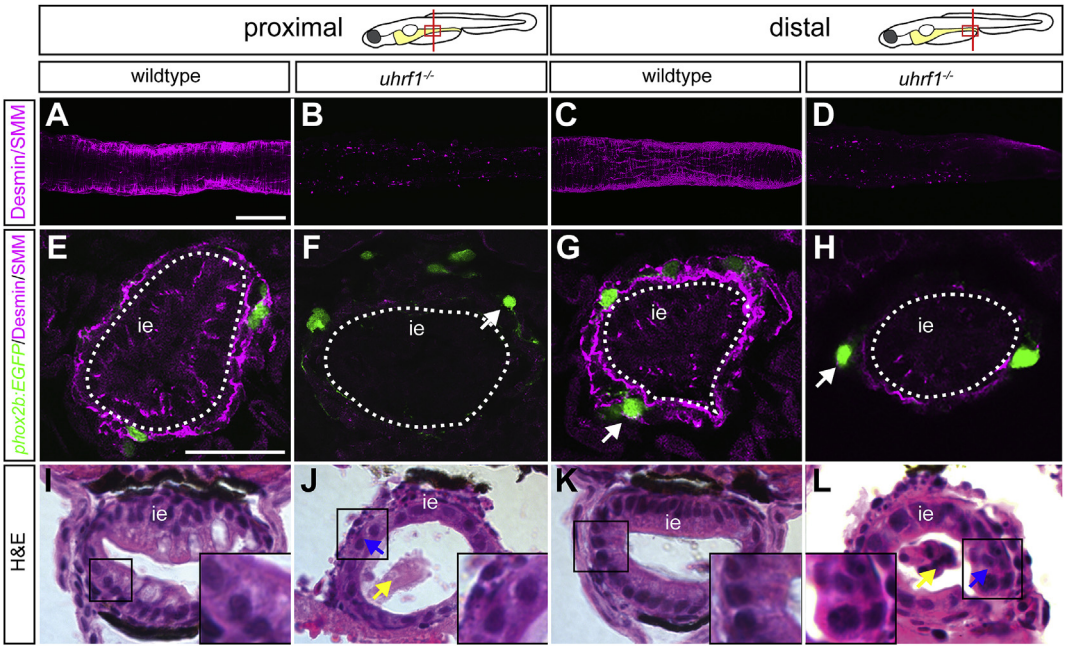

Fig. 8. Disrupted smooth muscle development contributes to intestinal dysgenesis in *uhrf1* mutants. Confocal images of 5 dpf intestines labeled with smooth muscle myosin (SMM) and desmin (magenta) antibodies. Dissected intestines (A–D) of wildtype (A,C) and *uhrf1* mutants (B,D). In both proximal (B) and distal (D) intestine, *uhrf1* mutants essentially lack smooth muscle cells, as revealed by whole-mount antibody staining. Transverse sections of wildtype (E,G) and *uhrf1* mutants (F,H) showing loss of intestinal smooth muscle in mutants. White arrows point to *phox2b:EGFP* (green) positive ENS neurons that are further removed from the intestinal epithelium in mutants (F,H) than in wildtypes (G). Brightfield images of transverse sections of 5 dpf wildtypes (I,K) and *uhrf1* mutants (J,L) stained with hematoxylin and eosin show disrupted proximal and distal intestinal development in mutants compared to wildtypes. Increased shedding of cells in *uhrf1* mutants is indicated by a yellow arrow and disrupted intestinal epithelium with a blue arrow. Higher magnification insets of boxed areas indicate disrupted intestinal epithelium morphology in *uhrf1* mutants. ie = intestinal epithelium. Scale bar = 50 µm in A-D, and 25 µm in E-L.

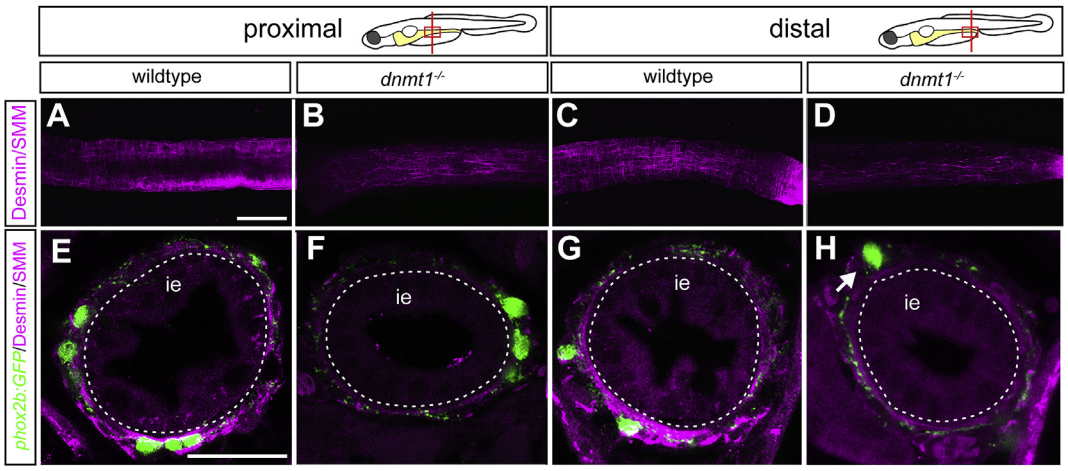

Fig. 9. Disrupted smooth muscle development contributes to intestinal dysgenesis in *dnmt1* mutants. Confocal images of 5 dpf intestines labeled with smooth muscle myosin (SMM) and desmin (magenta) antibodies. Dissected intestines (A–D) of wildtype (A,C) and *dnmt1* mutants (B,D). In both proximal (B) and distal (D) intestine, *dnmt1* mutants essentially lack smooth muscle cells, as revealed by whole-mount antibody staining. Transverse sections of wildtype (E,G) and *dnmt1* mutants (F,H) showing loss of intestinal smooth muscle in mutants. White arrow points to *phox2b:EGFP* (green) positive ENS neuron that is further removed from the intestinal epithelium in mutants (H) than in wildtypes (G). ie = intestinal epithelium. Scale bar = 50 μm in A-D, and 25 μm in E-H.

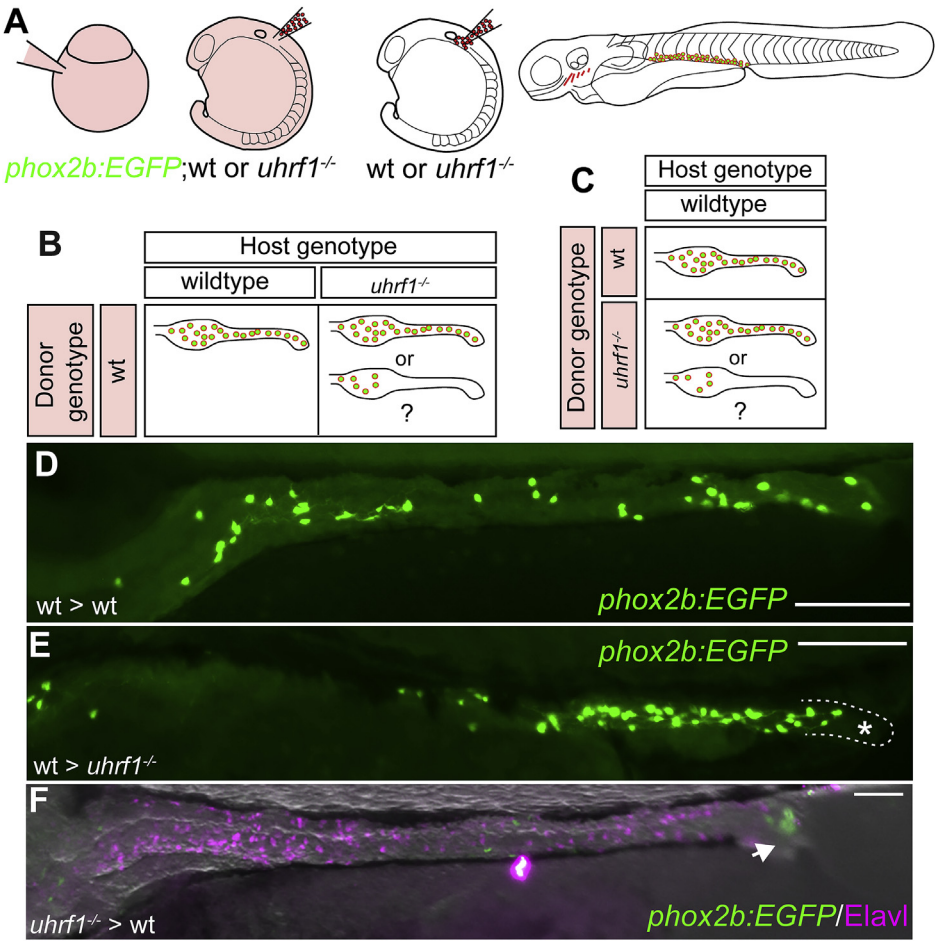

Fig. 10. Genetic chimeras reveal that Uhrf1 functions cell-non-autonomously and cell-autonomously in ENS development. (A) Transplantation experiment diagram. Wildtype or *uhrf1* mutant donor embryos that carry the *phox2b:EGFP* transgene were injected with rhodamine dextran. Vagal neural crest cells were transplanted from donors into unlabeled wildtype or *uhrf1* mutant hosts. The contribution of transplanted cells was evaluated at 5 dpf. (B) Possible results for transplantation experiments to test cell-non-autonomous function of *uhrf1* in ENS development. (C) Possible results for transplantation experiments to test cell-autonomous function of *uhrf1* in ENS development. (D) *phox2b:EGFP* positive (green) wildtype cells transplanted into wildtype hosts can populate the entire intestine. Note that the density of these cells is less than in non-transplanted animals because they share the territory with unlabeled ENS cells of the host. (E) *phox2b:EGFP* positive (green) wildtype cells transplanted into *uhrf1* mutant hosts can expand, but are consistently excluded from distal intestine (outlined and labeled with asterisk). (F) *phox2b:EGFP* positive (green) *uhrf1* mutant cells transplanted into wildtype hosts can migrate to distal intestine in rare cases (1/5), but the population of transplanted mutant cells that successfully integrate into the ENS is smaller than that of the wildtype host cells as revealed by Elavl staining (magenta). (D–F) Lateral views of whole-mount zebrafish larvae at 5 dpf. Scale bar = 100 μm in D-F.

et al., 2007, 2013; Olden et al., 2008; Pietsch et al., 2006; Puzan et al., 2018; Reichenbach et al., 2008; Sukegawa et al., 2000), making it difficult to discern which cell types require DNA methylation factor function for their differentiation. Mouse *Uhrf1* mutants die early, before the intestine develops (Bostick et al., 2007; Muto et al., 2002; Sharif et al., 2007), and so mouse does not serve as a model in which to investigate the role of Uhrf1 in intestinal development. In contrast, zebrafish *uhrf1* mutants survive to larval stages due to maternally provided Uhrf1 protein (Jacob et al., 2015), thus the role of *uhrf1* in intestinal development can be investigated. Below we discuss the role of methylation factors in the context of intestinal disease and coordinated intestinal development.

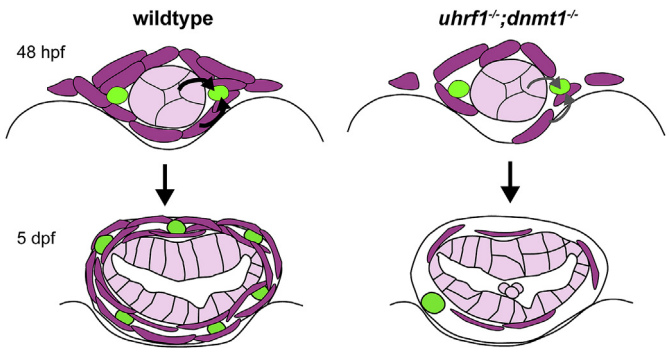

Fig. 11. Model of Uhrf1 and Dnmt1 function during ENS development. Signaling is important for differentiation of intestinal cells derived from each of the germ layers. We showed that during early intestinal development, Uhrf1 and Dnmt1 have cell-autonomous functions in EPCs (green), but that EPC development is also affected cell-non-autonomously, probably as a result of Uhrf1 and Dnmt1 functions in surrounding intestinal epithelial cells (light pink) and smooth muscle cells (purple). Together these cell-autonomous and cell-non-autonomous Uhrf1 and Dnmt1 activities modulate ENS development. This diagram shows signaling from epithelial and muscle precursors to ENS precursors. Decreasing these signals in *uhrf1* and *dnmt1* mutants (lighter arrows) results in fewer smooth muscle and epithelial progenitors, and thus alters proliferation, migration, or differentiation of EPCs, potentially also contributing to EPC death. Although not shown here, it is also likely that cell-autonomous and cell-non-autonomous functions of these genes modulate intestinal epithelial and muscle cell development.

4.1. Dysregulation of Uhrf1 and Dnmt1 are linked to intestinal diseases

Epigenetic regulation of gene expression has been implicated in a variety of types of diseases that affect development of the intestinal tract (Anderson et al., 2009; Feng et al., 2010). For example, Uhrf1 mutations cause dysregulation of the intestinal epithelium in a zebrafish model of inflammatory bowel disease (IBD) (Marjoram et al., 2015). DNMT1 has been shown to be dysregulated in human Crohn's disease, one type of IBD, (Jorgensen et al., 2018). *Dnmt1* mutations engineered to be present solely in mouse intestinal smooth muscle cells cause muscle hypoproliferation and decreased intestinal peristalsis, phenotypes found in human diseases such as chronic intestinal pseudo-obstruction and megacystis-megacolon-intestinal hypoperistalsis syndrome (Jorgensen et al., 2018). DNA hypomethylation, due at least in some case to mutations in DNMT3, has also been linked to human HSCR and Waardenburg syndrome (Kim et al., 2011; Torroglosa et al., 2014, 2016). In addition, epigenetic modulation of methylation is associated with other types of intestinal diseases, such as intestinal cancers (Gays et al., 2017).

In some cases, these intestinal diseases result from mutations that specifically affect cells in one of the germ layers that contributes to the developing intestinal tract. For example, HSCR results from failure of normal ENS development. Changes in maintenance of DNA methylation can alter gene expression patterns and several HSCR loci including *RET*, *EDNRB*, and HSCR candidate genes, such as *PAX6*, have been shown to be affected by altered DNA methylation of their promoters (Torroglosa et al., 2016). A single nucleotide polymorphism (SNP) in a conserved non-coding element suggested to be a RET enhancer is associated with susceptibility to HSCR (Emison et al., 2005; Griseri et al., 2005). Thus, SNPs in *uhrf1* and *dnmt1* enhancers driving expression in ENS cells could specifically affect ENS development, leading to HSCR-like phenotypes, while not directly affecting other intestinal cell types.

Although mutations in intestinal cells derived from a specific germ layer may cause disease, because of the intimate interactions among cells of these germ layers, mutations in more globally acting genes may have both cell-autonomous and cell-non-autonomous effects. For example, in the study by Marjoram et al. (2015), mutations in *uhrf1* or *dnmt1* resulted in hypoproliferation and excess shedding of epithelial cells into the intestinal lumen in their IBD model. However, these mutations were throughout the organism, including all cells of the intestinal tract, but contributions to the observed phenotype from intestinal smooth muscle or ENS progenitors were not examined. The ENS has been implicated in regulating intestinal barrier function (Neunlist et al., 2013; Sharkey, 2015), suggesting that the ENS phenotype observed in our study could be a contributing factor to compromised intestinal barrier function in *uhrf1* mutants.

4.2. Uhrf1 and Dnmt1 promote coordinated intestinal development

Development of a functional intestine is the result of highly orchestrated processes (Fig. 11). Each of the contributing germ layers must be specified and component cells must segregate and migrate to their appropriate destinations (Ganz, 2018; Ganz et al., 2016; Hao et al., 2016; Wallace et al., 2005a). Endoderm reaches the midline early and forms a scaffold for the incoming mesoderm that migrates from the lateral plate (Gays et al., 2017). In contrast, ectoderm-derived neural crest cells first migrate ventrally to the nascent intestine and then migrate from rostral to caudal along the developing intestinal epithelium and mesoderm. All of these processes occur within a fairly narrow time window during which each cell type also proliferates, a process that has been best studied for the ENS (Shepherd and Eisen, 2011). In the ENS, migration and proliferation are intimately connected; decreased proliferation leads to decreased migration and vice versa (Landman et al., 2007; Nagy and Goldstein, 2017; Newgreen et al., 2017; Simpson et al., 2007). Uhrf1 and Dnmt1 mutations block the cell cycle, leading to fewer cells in the affected tissue or organ (Jacob et al., 2015), providing a potential mechanism for the decreased number of ENS neurons in these mutants. A similar mechanism may be at play in intestinal smooth muscle and intestinal epithelium, although this hypothesis remains to be tested.

Because each of the intestinal cell types independently fail to form properly in *dnmt1* and *uhrf1* mutants, signals produced by that cell type necessary for differentiation of the other two cell types decrease. Consistent with this idea, zebrafish mutants that exhibit decreased intestinal smooth muscle cell development also show ENS abnormalities (Wallace et al., 2005a). Mutations in genes involved in methylation can lead to premature differentiation (Sen et al., 2010), which would decrease the number of cells, leading to decreased migration and thus a diminution of signals important for adjacent cell types to differentiate. Premature differentiation and aberrant migration of EPCs, ISMPs, or intestinal epithelial progenitor cells would likely decrease inter-germ layer signaling. Thus, prematurely differentiating cells might receive and send incorrect signals to neighboring cells, leading to differentiated cells that become inappropriately specified. Another possibility is that progenitor or differentiated intestinal cells might die prematurely in these mutants, potentially because they are mis-specified. Such premature death would also lead to fewer cells providing diminished inter-germ layer signaling. Cell type specific knock-outs of *uhrf1* and *dnmt1*, as well as time-lapse live imaging studies, would help distinguish between these different mechanisms.

Our transplantation experiments provide evidence that methylation factors act both cell-autonomously and cell-non-autonomously in the ENS. Given the expression patterns of the genes encoding these factors, this is not surprising. Thus, we suggest that this is also likely to be the case in intestinal smooth muscle and epithelium. This hypothesis can be tested by creating genetic chimeras for these cell populations or by cell type specific knock-outs.

Conflicts of interest

No competing interests declared.

Author contributions (CRediT taxonomy)

Conceptualization: JSE, JG, EM.
Methodology: JSE, JG, EM, AA, CW, JHP.

Validation: JG, EM, AA, CW, JHP, MS, PB, IB.
Formal analysis: JG, EM, AA, CW, JHP, MS, PB, IB, JSE.
Investigation: JG, EM, AA, CW, PB, MS, IB, PD, JK, JHP, JSE.
Resources: JSE, JHP, JG.
Data curation: CW, EM, JG, JSE.
Writing-original draft preparation: JG, EM, JSE.
Writing-review and editing: JG, EM, AA, CW, PB, MS, IB, PD, JK, JHP, JSE.
Visualization: EM, JG, JSE.
Project administration: JSE.
Funding acquisition: JSE, JHP, JG.
Mutant mapping: EM, JG, AA, CW, PB, IB.

Acknowledgments

We thank Doug Turnbull and the University of Oregon Genomics and Cell Characterization Core Facility for their expertise in Illumina sequencing and bioinformatics, Kirsten Sadler Edepli and her laboratory for the *uhrf1* plasmid, Poh Kheng Loi for histology, Adam Christensen, John Dowd, Markus Melancon, and the UO Zebrafish Facility staff for zebrafish husbandry. This work was supported by NIH P01 HD22486, NIH R01 OD11116, and by a research grant from the REACHirschsprung foundation to J.G.

References

Amores, A., Catchen, J., Ferrara, A., Fontenot, Q., Postlethwait, J.H., 2011. Genome evolution and meiotic maps by massively parallel DNA sequencing: spotted gar, an outgroup for the teleost genome duplication. Genetics 188, 799–808.
Amsterdam, A., Hopkins, N., 2004. Retroviral-mediated insertional mutagenesis in zebrafish. Methods Cell Biol. 77, 3–20.
Anderson, R.M., Bosch, J.A., Goll, M.G., Hesselson, D., Dong, P.D., Shin, D., Chi, N.C., Shin, C.H., Schlegel, A., Halpern, M., Stainier, D.Y., 2009. Loss of Dnmt1 catalytic activity reveals multiple roles for DNA methylation during pancreas development and regeneration. Dev. Biol. 334, 213–223.
Baird, N.A., Etter, P.D., Atwood, T.S., Currey, M.C., Shiver, A.L., Lewis, Z.A., Selker, E.U., Cresko, W.A., Johnson, E.A., 2008. Rapid SNP discovery and genetic mapping using sequenced RAD markers. PLoS One 3, e3376.
Beattie, C.E., Eisen, J.S., 1997. Notochord alters the permissiveness of myotome for pathfinding by an identified motoneuron in embryonic zebrafish. Development 124, 713–720.
Bestor, T.H., 2000. The DNA methyltransferases of mammals. Hum. Mol. Genet. 9, 2395–2402.
Borden, K.L., Freemont, P.S., 1996. The RING finger domain: a recent example of a sequence-structure family. Curr. Opin. Struct. Biol. 6, 395–401.
Bostick, M., Kim, J.K., Esteve, P.O., Clark, A., Pradhan, S., Jacobsen, S.E., 2007. UHRF1 plays a role in maintaining DNA methylation in mammalian cells. Science 317, 1760–1764.
Brosens, E., Burns, A.J., Brooks, A.S., Matera, I., Borrego, S., Ceccherini, I., Tam, P.K., Garcia-Barcelo, M.M., Thapar, N., Benninga, M.A., Hofstra, R.M., Alves, M.M., 2016. Genetics of enteric neuropathies. Dev. Biol. 417, 198–208.
Catchen, J., Bassham, S., Wilson, T., Currey, M., O'Brien, C., Yeates, Q., Cresko, W.A., 2013. The population structure and recent colonization history of Oregon threespine stickleback determined using restriction-site associated DNA-sequencing. Mol. Ecol. 22, 2864–2883.
Catchen, J.M., Amores, A., Hohenlohe, P., Cresko, W., Postlethwait, J.H., 2011. Stacks: building and genotyping Loci de novo from short-read sequences. G3 (Bethesda) 1, 171–182.
Cheesman, S.E., Neal, J.T., Mittge, E., Seredick, B.M., Guillemin, K., 2011. Epithelial cell proliferation in the developing zebrafish intestine is regulated by the Wnt pathway and microbial signaling via Myd88. Proc. Natl. Acad. Sci. U. S. A. 108 (Suppl. 1), 4570–4577.
Eisen, J.S., 1991. Determination of primary motoneuron identity in developing zebrafish embryos. Science 252, 569–572.
Elliott, E.N., Kaestner, K.H., 2015. Epigenetic regulation of the intestinal epithelium. Cell. Mol. Life Sci. 72, 4139–4156.
Elliott, E.N., Sheaffer, K.L., Schug, J., Stappenbeck, T.S., Kaestner, K.H., 2015. Dnmt1 is essential to maintain progenitors in the perinatal intestinal epithelium. Development 142, 2163–2172.
Emison, E.S., McCallion, A.S., Kashuk, C.S., Bush, R.T., Grice, E., Lin, S., Portnoy, M.E., Cutler, D.J., Green, E.D., Chakravarti, A., 2005. A common sex-dependent mutation in a RET enhancer underlies Hirschsprung disease risk. Nature 434, 857–863.
Feng, S., Cokus, S.J., Zhang, X., Chen, P.Y., Bostick, M., Goll, M.G., Hetzel, J., Jain, J., Strauss, S.H., Halpern, M.E., Ukomadu, C., Sadler, K.C., Pradhan, S., Pellegrini, M., Jacobsen, S.E., 2010. Conservation and divergence of methylation patterning in plants and animals. Proc. Natl. Acad. Sci. U. S. A. 107, 8689–8694.
Fu, M., Lui, V.C., Sham, M.H., Pachnis, V., Tam, P.K., 2004. Sonic hedgehog regulates the proliferation, differentiation, and migration of enteric neural crest cells in gut. J. Cell Biol. 166, 673–684.
Ganz, J., 2018. Gut feelings: studying enteric nervous system development, function, and disease in the zebrafish model system. Dev. Dynam. 247, 268–278.
Ganz, J., Melancon, E., Eisen, J.S., 2016. Zebrafish as a model for understanding enteric nervous system interactions in the developing intestinal tract. Methods Cell Biol. 134, 139–164.
Gays, D., Hess, C., Camporeale, A., Ala, U., Provero, P., Mosimann, C., Santoro, M.M., 2017. An exclusive cellular and molecular network governs intestinal smooth muscle cell differentiation in vertebrates. Development 144, 464–478.
Goldstein, A.M., Thapar, N., Karunaratne, T.B., De Giorgio, R., 2016. Clinical aspects of neurointestinal disease: pathophysiology, diagnosis, and treatment. Dev. Biol. 417, 217–228.
Graham, H.K., Maina, I., Goldstein, A.M., Nagy, N., 2017. Intestinal smooth muscle is required for patterning the enteric nervous system. J. Anat. 230, 567–574.
Griseri, P., Bachetti, T., Puppo, F., Lantieri, F., Ravazzolo, R., Devoto, M., Ceccherini, I., 2005. A common haplotype at the 5' end of the RET proto-oncogene, overrepresented in Hirschsprung patients, is associated with reduced gene expression. Hum. Mutat. 25, 189–195.
Hao, M.M., Foong, J.P., Bornstein, J.C., Li, Z.L., Vanden Berghe, P., Boesmans, W., 2016. Enteric nervous system assembly: functional integration within the developing gut. Dev. Biol. 417, 168–181.
Heuckeroth, R.O., 2018. Hirschsprung disease - integrating basic science and clinical medicine to improve outcomes. Nat. Rev. Gastroenterol. Hepatol. 15, 152–167.
Hohenlohe, P.A., Bassham, S., Etter, P.D., Stiffler, N., Johnson, E.A., Cresko, W.A., 2010. Population genomics of parallel adaptation in threespine stickleback using sequenced RAD tags. PLoS Genet. 6, e1000862.
Howe, K., Clark, M.D., Torroja, C.F., Torrance, J., Berthelot, C., Muffato, M., Collins, J.E., Humphray, S., McLaren, K., Matthews, L., McLaren, S., Sealy, I., Caccamo, M., Churcher, C., Scott, C., Barrett, J.C., Koch, R., Rauch, G.J., White, S., Chow, W., Kilian, B., Quintais, L.T., Guerra-Assuncao, J.A., Zhou, Y., Gu, Y., Yen, J., Vogel, J.H., Eyre, T., Redmond, S., Banerjee, R., Chi, J., Fu, B., Langley, E., Maguire, S.F., Laird, G.K., Lloyd, D., Kenyon, E., Donaldson, S., Sehra, H., Almeida-King, J., Loveland, J., Trevanion, S., Jones, M., Quail, M., Willey, D., Hunt, A., Burton, J., Sims, S., McLay, K., Plumb, B., Davis, J., Clee, C., Oliver, K., Clark, R., Riddle, C., Elliot, D., Threadgold, G., Harden, G., Ware, D., Begum, S., Mortimore, B., Kerry, G., Heath, P., Phillimore, B., Tracey, A., Corby, N., Dunn, M., Johnson, C., Wood, J., Clark, S., Pelan, S., Griffiths, G., Smith, M., Glithero, R., Howden, P., Barker, N., Lloyd, C., Stevens, C., Harley, J., Holt, K., Panagiotidis, G., Lovell, J., Beasley, H., Henderson, C., Gordon, D., Auger, K., Wright, D., Collins, J., Raisen, C., Dyer, L., Leung, K., Robertson, L., Ambridge, K., Leongamornlert, D., McGuire, S., Gilderthorp, R., Griffiths, C., Manthravadi, D., Nichol, S., Barker, G., Whitehead, S., Kay, M., Brown, J., Murnane, C., Gray, E., Humphries, M., Sycamore, N., Barker, D., Saunders, D., Wallis, J., Babbage, A., Hammond, S., Mashreghi-Mohammadi, M., Barr, L., Martin, S., Wray, P., Ellington, A., Matthews, N., Ellwood, M., Woodmansey, R., Clark, G., Cooper, J., Tromans, A., Grafham, D., Skuce, C., Pandian, R., Andrews, R., Harrison, E., Kimberley, A., Garnett, J., Fosker, N., Hall, R., Garner, P., Kelly, D., Bird, C., Palmer, S., Gehring, I., Berger, A., Dooley, C.M., Ersan-Urun, Z., Eser, C., Geiger, H., Geisler, M., Karotki, L., Kirn, A., Konantz, J., Konantz, M., Oberlander, M., Rudolph-Geiger, S., Teucke, M., Lanz, C., Raddatz, G., Osoegawa, K., Zhu, B., Rapp, A., Widaa, S., Langford, C., Yang, F., Schuster, S.C., Carter, N.P., Harrow, J., Ning, Z., Herrero, J., Searle, S.M., Enright, A., Geisler, R., Plasterk, R.H., Lee, C., Westerfield, M., de Jong, P.J., Zon, L.I., Postlethwait, J.H., Nusslein-Volhard, C., Hubbard, T.J., Roest Crollius, H., Rogers, J., Stemple, D.L., 2013. The zebrafish reference genome sequence and its relationship to the human genome. Nature 496, 498–503.
Ignatius, M.S., Unal Eroglu, A., Malireddy, S., Gallagher, G., Nambiar, R.M., Henion, P.D., 2013. Distinct functional and temporal requirements for zebrafish Hdac1 during neural crest-derived craniofacial and peripheral neuron development. PLoS One 8, e63218.
Jacob, V., Chernyavskaya, Y., Chen, X., Tan, P.S., Kent, B., Hoshida, Y., Sadler, K.C., 2015. DNA hypomethylation induces a DNA replication-associated cell cycle arrest to block hepatic outgrowth in uhrf1 mutant zebrafish embryos. Development 142, 510–521.
Jorgensen, B.G., Berent, R.M., Ha, S.E., Horiguchi, K., Sasse, K.C., Becker, L.S., Ro, S., 2018. DNA methylation, through DNMT1, has an essential role in the development of gastrointestinal smooth muscle cells and disease. Cell Death Dis. 9, 474.
Kim, H., Kang, K., Ekram, M.B., Roh, T.Y., Kim, J., 2011. Aebp2 as an epigenetic regulator for neural crest cells. PLoS One 6, e25174.
Korzh, S., Winata, C.L., Zheng, W., Yang, S., Yin, A., Ingham, P., Korzh, V., Gong, Z., 2011. The interaction of epithelial Ihha and mesenchymal Fgf10 in zebrafish esophageal and swimbladder development. Dev. Biol. 359, 262–276.
Kuhlman, J., Eisen, J.S., 2007. Genetic screen for mutations affecting development and function of the enteric nervous system. Dev. Dynam. 236, 118–127.
Lake, J.I., Heuckeroth, R.O., 2013. Enteric nervous system development: migration, differentiation, and disease. Am. J. Physiol. Gastrointest. Liver Physiol. 305, G1–G24.
Landman, K.A., Simpson, M.J., Newgreen, D.F., 2007. Mathematical and experimental insights into the development of the enteric nervous system and Hirschsprung's disease. Dev. Growth Differ. 49, 277–286.
Liu, X., Jia, X., Yuan, H., Ma, K., Chen, Y., Jin, Y., Deng, M., Pan, W., Chen, S., Chen, Z., de The, H., Zon, L.I., Zhou, Y., Zhou, J., Zhu, J., 2015. DNA methyltransferase 1 functions through C/ebpa to maintain hematopoietic stem and progenitor cells in zebrafish. J. Hematol. Oncol. 8, 15.
Marjoram, L., Alvers, A., Deerhake, M.E., Bagwell, J., Mankiewicz, J., Cocchiaro, J.L., Beerman, R.W., Willer, J., Sumigray, K.D., Katsanis, N., Tobin, D.M., Rawls, J.F., Goll, M.G., Bagnat, M., 2015. Epigenetic control of intestinal barrier function and inflammation in zebrafish. Proc. Natl. Acad. Sci. U. S. A. 112, 2770–2775.
Miller, M.R., Atwood, T.S., Eames, B.F., Eberhart, J.K., Yan, Y.L., Postlethwait, J.H., Johnson, E.A., 2007. RAD marker microarrays enable rapid mapping of zebrafish mutations. Genome Biol. 8, R105.

Muto, M., Kanari, Y., Kubo, E., Takabe, T., Kurihara, T., Fujimori, A., Tatsumi, K., 2002. Targeted disruption of Np95 gene renders murine embryonic stem cells hypersensitive to DNA damaging agents and DNA replication blocks. J. Biol. Chem. 277, 34549–34555.
Mwizerwa, O., Das, P., Nagy, N., Akbareian, S.E., Mably, J.D., Goldstein, A.M., 2011. Gdnf is mitogenic, neurotrophic, and chemoattractive to enteric neural crest cells in the embryonic colon. Dev. Dynam. 240, 1402–1411.
Nagy, N., Goldstein, A.M., 2017. Enteric nervous system development: a crest cell's journey from neural tube to colon. Semin. Cell Dev. Biol. 66, 94–106.
Natarajan, D., Marcos-Gutierrez, C., Pachnis, V., de Graaff, E., 2002. Requirement of signalling by receptor tyrosine kinase RET for the directed migration of enteric nervous system progenitor cells during mammalian embryogenesis. Development 129, 5151–5160.
Nechiporuk, A., Linbo, T., Poss, K.D., Raible, D.W., 2007. Specification of epibranchial placodes in zebrafish. Development 134, 611–623.
Neunlist, M., Aubert, P., Bonnaud, S., Van Landeghem, L., Coron, E., Wedel, T., Naveilhan, P., Ruhl, A., Lardeux, B., Savidge, T., Paris, F., Galmiche, J.P., 2007. Enteric glia inhibit intestinal epithelial cell proliferation partly through a TGF-beta1-dependent pathway. Am. J. Physiol. Gastrointest. Liver Physiol. 292, G231–G241.
Neunlist, M., Van Landeghem, L., Mahe, M.M., Derkinderen, P., des Varannes, S.B., Rolli-Derkinderen, M., 2013. The digestive neuronal-glial-epithelial unit: a new actor in gut health and disease. Nat. Rev. Gastroenterol. Hepatol. 10, 90–100.
Newgreen, D.F., Zhang, D., Cheeseman, B.L., Binder, B.J., Landman, K.A., 2017. Differential clonal expansion in an invading cell population: clonal advantage or dumb luck? Cells Tissues Organs 203, 105–113.
Olden, T., Akhtar, T., Beckman, S.A., Wallace, K.N., 2008. Differentiation of the zebrafish enteric nervous system and intestinal smooth muscle. Genesis 46, 484–498.
Ooi, S.K., Bestor, T.H., 2008. Cytosine methylation: remaining faithful. Curr. Biol. 18, R174–R176.
Pietsch, J., Delalande, J.M., Jakaitis, B., Stensby, J.D., Dohle, S., Talbot, W.S., Raible, D.W., Shepherd, I.T., 2006. Lessen encodes a zebrafish trap100 required for enteric nervous system development. Development 133, 395–406.
Puzan, M., Hosic, S., Ghio, C., Koppes, A., 2018. Enteric nervous system regulation of intestinal stem cell differentiation and epithelial monolayer function. Sci. Rep. 8, 6313.
Rai, K., Nadauld, L.D., Chidester, S., Manos, E.J., James, S.R., Karpf, A.R., Cairns, B.R., Jones, D.A., 2006. Zebra fish Dnmt1 and Suv39h1 regulate organ-specific terminal differentiation during development. Mol. Cell. Biol. 26, 7077–7085.
Reichenbach, B., Delalande, J.M., Kolmogorova, E., Prier, A., Nguyen, T., Smith, C.M., Holzschuh, J., Shepherd, I.T., 2008. Endoderm-derived Sonic hedgehog and mesoderm Hand2 expression are required for enteric nervous system development in zebrafish. Dev. Biol. 318, 52–64.
Robertson, K.D., Wolffe, A.P., 2000. DNA methylation in health and disease. Nat. Rev. Genet. 1, 11–19.
Rolig, A.S., Mittge, E.K., Ganz, J., Troll, J.V., Melancon, E., Wiles, T.J., Alligood, K., Stephens, W.Z., Eisen, J.S., Guillemin, K., 2017. The enteric nervous system promotes intestinal health by constraining microbiota composition. PLoS Biol. 15, e2000689.
Sadler, K.C., Krahn, K.N., Gaur, N.A., Ukomadu, C., 2007. Liver growth in the embryo and during liver regeneration in zebrafish requires the cell cycle regulator, uhrf1. Proc. Natl. Acad. Sci. U. S. A. 104, 1570–1575.
Sen, G.L., Reuter, J.A., Webster, D.E., Zhu, L., Khavari, P.A., 2010. DNMT1 maintains progenitor function in self-renewing somatic tissue. Nature 463, 563–567.
Seredick, S.D., Van Ryswyk, L., Hutchinson, S.A., Eisen, J.S., 2012. Zebrafish Mnx proteins specify one motoneuron subtype and suppress acquisition of interneuron characteristics. Neural Dev. 7, 35.
Sharif, J., Muto, M., Takebayashi, S., Suetake, I., Iwamatsu, A., Endo, T.A., Shinga, J., Mizutani-Koseki, Y., Toyoda, T., Okamura, K., Tajima, S., Mitsuya, K., Okano, M., Koseki, H., 2007. The SRA protein Np95 mediates epigenetic inheritance by recruiting Dnmt1 to methylated DNA. Nature 450, 908–912.
Sharkey, K.A., 2015. Emerging roles for enteric glia in gastrointestinal disorders. J. Clin. Investig. 125, 918–925.
Sheaffer, K.L., Kim, R., Aoki, R., Elliott, E.N., Schug, J., Burger, L., Schubeler, D., Kaestner, K.H., 2014. DNA methylation is required for the control of stem cell differentiation in the small intestine. Genes Dev. 28, 652–664.
Shepherd, I., Eisen, J., 2011. Development of the zebrafish enteric nervous system. Methods Cell Biol. 101, 143–160.
Shepherd, I.T., Pietsch, J., Elworthy, S., Kelsh, R.N., Raible, D.W., 2004. Roles for GFRalpha1 receptors in zebrafish enteric nervous system development. Development 131, 241–249.
Simpson, M.J., Zhang, D.C., Mariani, M., Landman, K.A., Newgreen, D.F., 2007. Cell proliferation drives neural crest cell invasion of the intestine. Dev. Biol. 302, 553–568.
Sukegawa, A., Narita, T., Kameda, T., Saitoh, K., Nohno, T., Iba, H., Yasugi, S., Fukuda, K., 2000. The concentric structure of the developing gut is regulated by Sonic hedgehog derived from endodermal epithelium. Development 127, 1971–1980.
Tauber, M., Fischle, W., 2015. Conserved linker regions and their regulation determine multiple chromatin-binding modes of UHRF1. Nucleus 6, 123–132.
Taylor, C.R., Montagne, W.A., Eisen, J.S., Ganz, J., 2016. Molecular fingerprinting delineates progenitor populations in the developing zebrafish enteric nervous system. Dev. Dynam. 245, 1081–1096.
Tittle, R.K., Sze, R., Ng, A., Nuckels, R.J., Swartz, M.E., Anderson, R.M., Bosch, J., Stainier, D.Y., Eberhart, J.K., Gross, J.M., 2011. Uhrf1 and Dnmt1 are required for development and maintenance of the zebrafish lens. Dev. Biol. 350, 50–63.
Torroglosa, A., Alves, M.M., Fernandez, R.M., Antinolo, G., Hofstra, R.M., Borrego, S., 2016. Epigenetics in ENS development and Hirschsprung disease. Dev. Biol. 417, 209–216.
Torroglosa, A., Enguix-Riego, M.V., Fernandez, R.M., Roman-Rodriguez, F.J., Moya-Jimenez, M.J., de Agustin, J.C., Antinolo, G., Borrego, S., 2014. Involvement of DNMT3B in the pathogenesis of Hirschsprung disease and its possible role as a regulator of neurogenesis in the human enteric nervous system. Genet. Med. 16, 703–710.
Troll, J.V., Hamilton, M.K., Abel, M.L., Ganz, J., Bates, J.M., Stephens, W.Z., Melancon, E., van der Vaart, M., Meijer, A.H., Distel, M., Eisen, J.S., Guillemin, K., 2018. Microbiota Promote Secretory Cell Determination in the Intestinal Epithelium by Modulating Host Notch Signaling, vol. 145. Development.
Uyttebroek, L., Shepherd, I.T., Harrisson, F., Hubens, G., Blust, R., Timmermans, J.P., Van Nassauw, L., 2010. Neurochemical coding of enteric neurons in adult and embryonic zebrafish (Danio rerio). J. Comp. Neurol. 518, 4419–4438.
Wallace, K.N., Akhter, S., Smith, E.M., Lorent, K., Pack, M., 2005a. Intestinal growth and differentiation in zebrafish. Mech. Dev. 122, 157–173.
Wallace, K.N., Dolan, A.C., Seiler, C., Smith, E.M., Yusuff, S., Chaille-Arnold, L., Judson, B., Sierk, R., Yengo, C., Sweeney, H.L., Pack, M., 2005b. Mutation of smooth muscle myosin causes epithelial invasion and cystic expansion of the zebrafish intestine. Dev. Cell 8, 717–726.
Warga, R.M., Nusslein-Volhard, C., 1999. Origin and development of the zebrafish endoderm. Development 126, 827–838.
Wu, T.D., Nacu, S., 2010. Fast and SNP-tolerant detection of complex variants and splicing in short reads. Bioinformatics 26, 873–881.
Yamamoto, H., Oda, Y., 2015. Gastrointestinal stromal tumor: recent advances in pathology and genetics. Pathol. Int. 65, 9–18.
Zorn, A.M., Wells, J.M., 2009. Vertebrate endoderm development and organ formation. Annu. Rev. Cell Dev. Biol. 25, 221–251.